JACS Au
AN OPEN ACCESS JOURNAL OF THE AMERICAN CHEMICAL SOCIETY

pubs.acs.org/jacsau
Article

Discovery of De Novo Macrocycle Inhibitors of Histone Deacetylase 11

Daniela Danková, Alexander L. Nielsen, Anne Zarda, Tobias N. Hansen, Marie Hesse, Michaela Benová, Athanasios Tsiris, Christian R. O. Bartling, Edward J. Will, Kristian Strømgaard, Carlos Moreno-Yruela, Christian Heinis,* and Christian A. Olsen*

Cite This: JACS Au 2025, 5, 1299−1307

ABSTRACT: Histone deacetylase (HDAC) enzymes are epigenetic regulators that affect diverse protein function by removing acyl groups from lysine side chains throughout the proteome. The most recently discovered human isozyme, HDAC11, differs from other HDACs in substrate preference and tissue expression profile. Elucidation of the biological function of this enzyme has been scarce and only a few chemical probes to help advance this insight have been developed thus far. Here we discovered macrocyclic inhibitors that exhibit selectivity for HDAC11 and penetrate the cytoplasmic membrane in cultured cells as determined by the chloroalkane penetration assay. Our work establishes the combination of de novo macrocycle synthesis with incorporation of *N*-alkylated hydroxamic acid moieties as a viable strategy for targeting HDAC11. Further, this study demonstrates the potential of applying macrocyclic peptide-based library synthesis to directly furnish high-affinity, cell-permeating ligands. The discovered inhibitors comprise tool compounds for the investigation of the biological function of HDAC11.

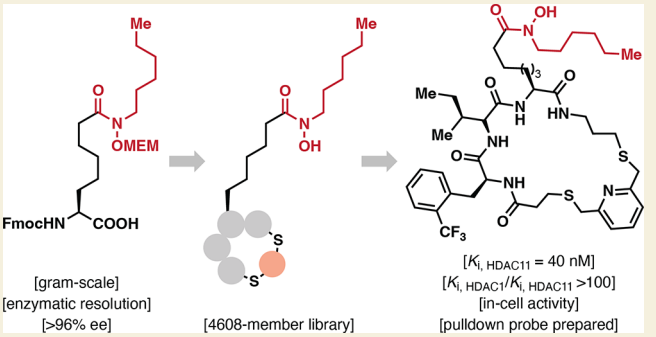

KEYWORDS: *posttranslational modification, lysine acylation, HDAC11, macrocycles, enzyme inhibitors*

INTRODUCTION

Histone deacetylase 11 (HDAC11) is the only Zn^{2+}-dependent HDAC enzyme that efficiently removes the long-chain acyl modification *ε*-*N*-myristoyllysine (Kmyr) from the side chains of lysine residues [>10,000-fold selectivity for Kmyr over *ε*-*N*-acetyllysine (Kac)].[1−3] The isozyme is the sole member in class IV of the human HDAC family and consists mostly of a catalytic domain with short N- and C-termini.[4] HDAC11 is highly conserved across species, but unlike most other HDACs, it is not universally expressed across tissues and is found primarily in brain, testis, and skeletal muscle. HDAC11 plays an integral role in immune response,[5] functioning as a transcriptional repressor of the key anti-inflammatory cytokine IL-10.[6,7] Furthermore, HDAC11 knockout mice resist weight gain on a high-fat diet and show better overall metabolic health, suggesting that HDAC11 could be a viable target for metabolic diseases.[8] Recently, the inhibition of HDAC11 has been shown to be a strategy for macrophage activation, highlighting the therapeutic potential for treatment of inflammation and for adaptive cell therapy.[9]

HDAC11 contains a catalytic Zn^{2+} ion in its substrate-binding pocket that can be targeted by different zinc-binding groups, which has formed the basis of a wide variety of HDAC inhibitors.[10−12] Naturally occurring macrocyclic peptides such as apicidin A and trapoxins A and B also contain zinc-binding groups and are generally potent inhibitors of class I HDACs.[13−18] Trapoxins and hydroxamic acid-containing analogs of these cyclic peptides, such as **apicidin A**$^{\mathbf{Asuha}}$, have also been shown to potently inhibit HDAC11, but to retain selectivity for class I HDACs[1] (Figure 1). To gain selectivity for HDAC11, we envisioned that the introduction of an alkyl group into the zinc-binding moiety would be preferentially accommodated in the active site of HDAC11, which efficiently catalyzes the hydrolysis of Kmyr. A similar strategy was reported for the development of HDAC11-selective small molecule inhibitors based on *N*-alkylated hydrazides (e.g., **SIS17**)[19] and was more recently applied to modify the epoxy ketone moiety of trapoxin A to improve selectivity for HDAC11 (**TD034**)[20] (Figure 1). The N-alkylation of hydroxamic acids, however, has not been applied in attempts to achieve selectivity for HDAC11; although, previously reported work has shown a decrease in affinity for class I

Received: November 27, 2024
Revised: January 23, 2025
Accepted: January 30, 2025
Published: February 16, 2025

https://doi.org/10.1021/jacsau.4c01148
JACS Au 2025, 5, 1299−1307

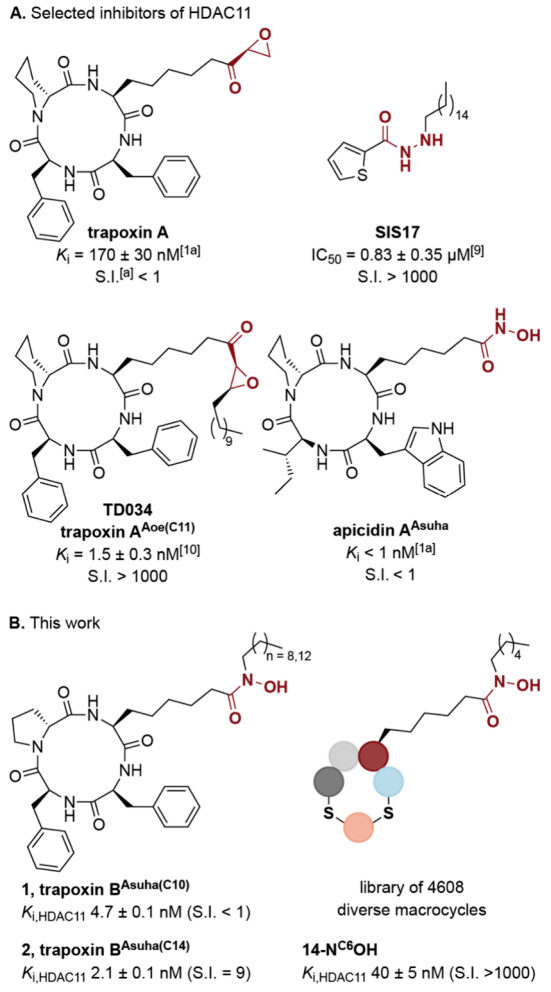

Figure 1. Structures of selected HDAC inhibitors. (A) Examples of previously identified inhibitors of HDAC11. (B) Natural product derived inhibitors and generic structure of macrocyclic library members prepared in this work. S.I. = selectivity index, defined as $K_{i,\ HDAC1}/K_{i,\ HDAC11}$.

HDACs.[21] These data led us to hypothesize that selectivity for HDAC11 could be induced by N-alkylation to disfavor class I HDAC targeting.

We initially synthesized two trapoxin B analogues (**1** and **2**) with N-alkylation of varying length at the nitrogen atom of the *S*-2-amino-8-(hydroxyamino)-suberic acid (Asuha) residue (Figure 1). The limited gain in selectivity observed (selectivity index HDAC11/HDAC1 < 10), combined with the limited aqueous solubility and challenging syntheses of these macrocycles, raised our concern for this strategy. Thus, instead of modifying privileged structures found in natural products, we embarked on high-throughput synthesis of a library of medium-sized cyclopeptide analogues, carrying an *N*-alkylated hydroxamic acid moiety to bias the library toward the binding pocket of HDAC11.

RESULTS AND DISCUSSION

Two different synthetic strategies were applied for the preparation of initial compounds **1** and **2**: *N*-decyl hydroxyl amine was coupled to a cyclic tetrapeptide precursor to deliver compound **1**, while an *N*-tetradecyl-containing amino acid building block was applied in the solid-phase peptide synthesis (SPPS) of a linear precursor, which followed by cyclization in solution furnished compound **2** (for full synthetic procedure, see the Supplementary Schemes S1 and S2). Both macrocycles were potent inhibitors of HDAC11 (K_i values of 4.7 nM and 2.1 nM, respectively) (Figure 1); however, compound **1** was an even more potent inhibitor of HDAC1 and compound **2** showed only a modest ∼9-fold selectivity for HDAC11 (Supplementary Figure S1 and Table S1). It has been shown that the trapoxin macrocycle contributes substantially to the binding affinity against class I HDACs,[18] which may hamper the use of these macrocycles for selective HDAC11 inhibition, at least in combination with hydroxamic acid−based warheads. We therefore turned to de novo high-throughput macrocycle library synthesis.

To allow for synthesis of libraries of several thousand macrocycles, a new amino acid building block carrying the modified zinc-binding group was warranted, because the *tert*-butyl protecting group, previously used for "SPOT" array

Scheme 1. Synthesis of Building Block 10[a]

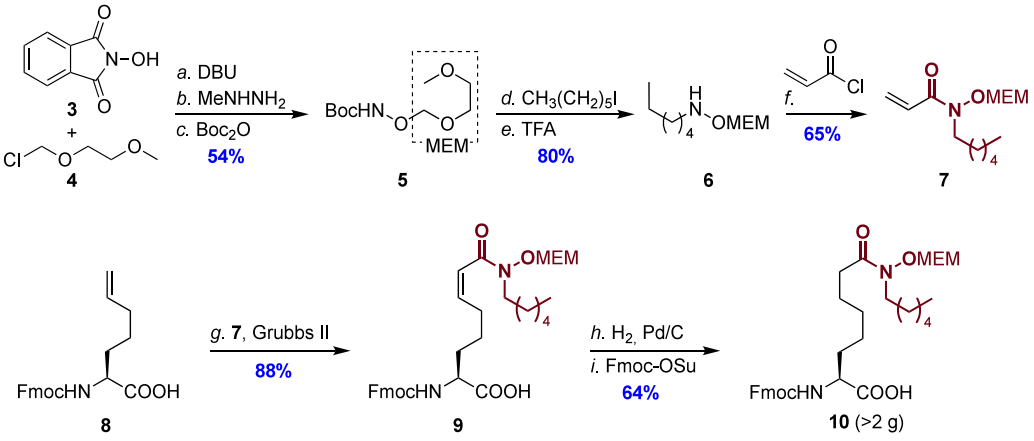

[a]Reagents and conditions: (a) MEM-Cl, 1,8-diazabicyclo[5.4.0]undec-7-ene (DBU), DMF, r.t., 16 h; (b) $MeNHNH_2$, CH_2Cl_2, r.t., 16 h; (c) Boc_2O, iPr_2NEt, 16 h; (d) 1-hexyl iodide, NaH, THF, 0 °C → r.t., 16 h; (e) TFA−CH_2Cl_2 (1:4), 1h; (f) acryloyl chloride, iPr_2NEt, CH_2Cl_2, 0 °C → r.t., 16 h; (g) Grubbs II catalyst (0.08 equiv), CH_2Cl_2, reflux, 5 h; (h) H_2, Pd/C (10% w/w) MeOH, r.t., 3 h; (i) Fmoc-OSu, iPr_2NEt, 1,4-dioxane, r.t., 16 h.

https://doi.org/10.1021/jacsau.4c01148
JACS Au 2025, 5, 1299−1307

Scheme 2. Synthesis of Macrocycle Library for Targeting HDAC11.[a]

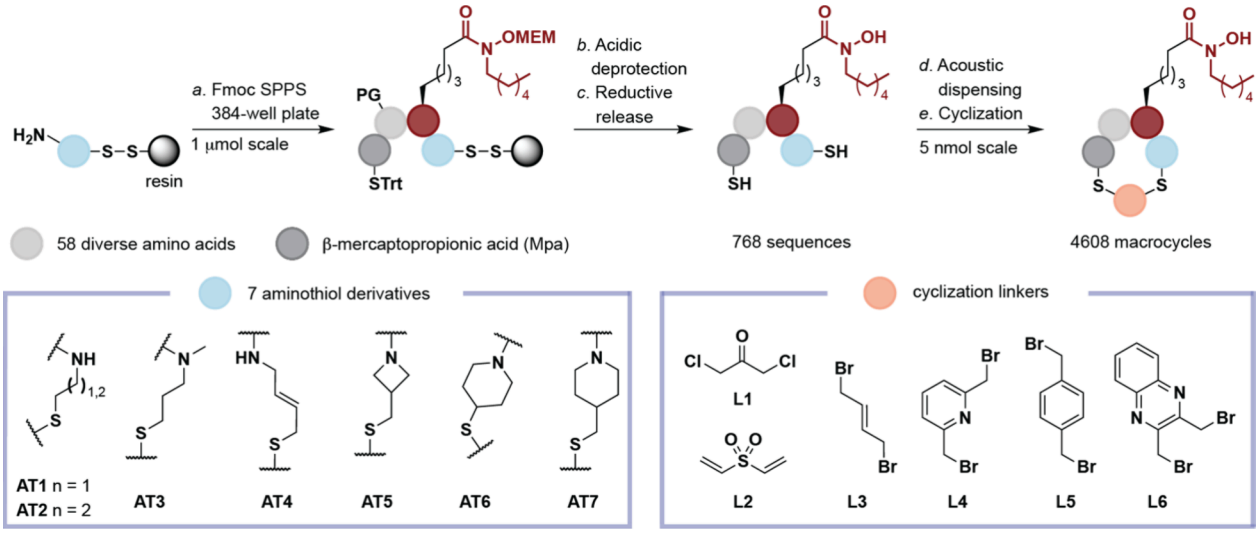

[a]Reagents and conditions: (a) (i) Fmoc-AA−OH, HATU, *N*-methylmorpholine, *N*-methyl-2-pyrrolidone (NMP), 2 h, 0.5 μmol scale (performed twice); (ii) piperidine−DMF (1:4), (2 × 2 min); (b) TFA−iPr$_3$SiH−H$_2$O (95:2.5:2.5); (c) 1,4-butanedithiol, Et$_3$N, DMF, 5 h, 5 nmol scale; (d) Reconstitution in DMSO and acoustic dispensing into 1536-well microtiter plates; (e) (i) bis-eletrophile (**L2**−**L6**), NH$_4$HCO$_3$, MeCN−H$_2$O (1:1, v/v, pH 8), 2 h; (ii) β-mercaptoethanol quenching. For full lists of employed amino acid building blocks and synthesized compounds, please consult Supplementary Table S5.

synthesis on cellulose membranes,[22] was incompatible with the high-throughput SPPS method. The *tert*-butyl group was replaced by a more acid labile methoxy ethoxymethyl (MEM) group that could be removed by the standard SPPS cleavage cocktails [containing 95% trifluoroacetic acid (TFA)]. Because of our experience with the limited solubility of the *N*-tetradecyl-modified trapoxin B analogue, we reasoned that a shorter alkyl chain would lead to better overall physicochemical properties of the macrocycles in the library, while still providing some bias toward inhibiting HDAC11 over other HDACs. Thus, we designed an *N*-hexyl, *O*-MEM-modified Asuha building block (**10**), which was synthesized in five steps, with a Grubbs cross-metathesis between the MEM-protected acryloyl hydroxamic acid building block (**7**) and 9-fluorenylethyloxycarbonyl (Fmoc) protected pentenyl glycine (**8**) as the key step (Scheme 1). Subsequent reduction of the formed olefin and reintroduction of the Fmoc group, which was partially cleaved during hydrogenation, furnished the desired amino acid (**10**) on gram-scale in 16% overall yield.

With building block **10** in hand, we synthesized a library of small, structurally diverse macrocycles, containing the *N*-alkylated Asuha residue as an HDAC-binding anchor, in a high-throughput and purification free manner (Scheme 2). The intermediate 768 linear dithiol-containing peptides were synthesized by SPPS in 384-well plates by employing a series of seven aminothiols as the initial building blocks linked via disulfide bonds to the solid support.[23,24] The disulfides are stable to TFA treatment, which is used to remove side chain protecting groups upon synthesis of the resin-bound library members. The resulting 768 peptides were released from the solid support by reductive cleavage using 1,4-butanedithiol (BDT)[25] to give linear bis-thiol compounds, containing two or three amino acids with β-mercaptopropionic acid (Mpa) at the N-terminus (Scheme 2). The library members were synthesized in good overall purity; although, with varying amounts of MEM-protected peptides observed (M+88) due to incomplete deprotection of the hydroxamate when performing the syntheses in plate format (Supplementary Figure S5 and S6). This observation was not in line with our previous tests on the stability of the MEM group in 95% TFA (Supplementary Figure S2) but was deemed acceptable for screening purposes, because of the inert character of the protected peptides with respect to binding to the Zn^{2+} ion in the active site of the HDACs. The linear peptides were then cyclized by a series of bis-electrophiles in 1536-well plates (Scheme 2) using automated liquid handling and acoustic droplet ejection technology (see Supplementary Figure S3 for workflow).[26,27] High structural diversity was achieved by introducing multiple diversifying elements: seven different aminothiols (ATs) with varying levels of flexibility were introduced at the C-terminus, 58 diverse amino acids were selected, and cyclization was performed with six different linkers in the final compounds (Scheme 2 and Supplementary Table S4 and S5). This automated synthesis afforded a library of 4608 macrocycles for high-throughput screening in vitro.

While there are several types of assays available for screening of potential inhibitors of HDAC11,[28] the methods based on HPLC analysis[2,3] are not readily applicable for high-throughput screening. We therefore adapted a fluorogenic HDAC11 assay that was previously developed in our laboratory,[1,29] which we optimized for fully automated 1536-well plate screening. The library was screened against HDAC11 at 2 μM concentration of the crude inhibitors and 12 hits, which inhibited the enzyme to <60% the residual activity, were selected for further investigation (Figure 2A and Supplementary Table S6).

Structure−activity relationship (SAR) analysis revealed a preference for hydrophobic residues, such as allylglycine (AllylG), α-L-aminobutyric acid (Abu), β-homoalanine (β-hAla), methionine (Met), and various analogues of phenylalanine (Phe), while few polar residues were accommodated in the hits. Thus, these data suggest that inhibitors, which display hydrophobic functionalities toward the proximity of the binding pocket preferentially target HDAC11. Most residues

https://doi.org/10.1021/jacsau.4c01148
JACS Au 2025, 5, 1299−1307

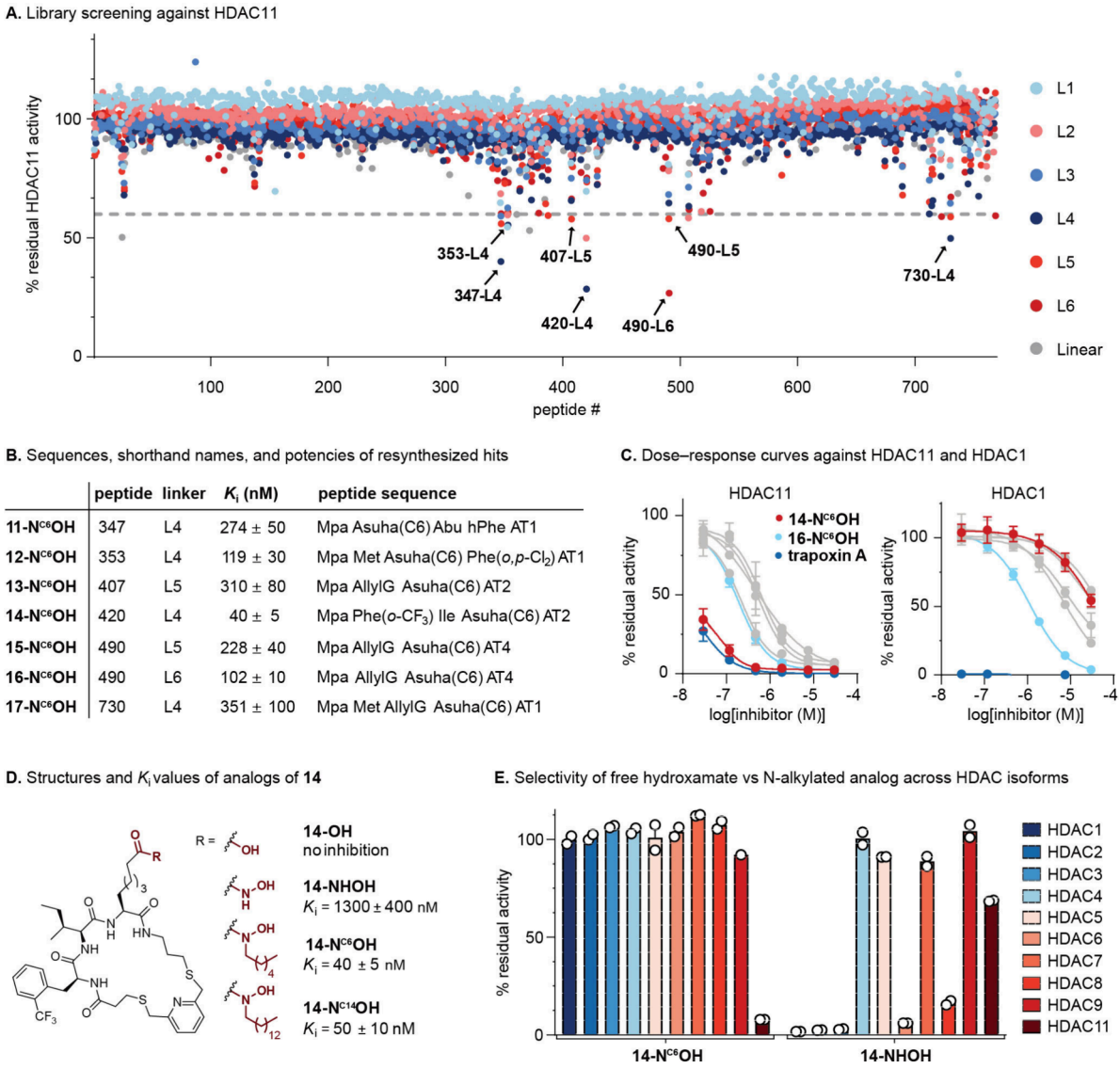

Figure 2. Macrocyclic library screening, hit validation, and selectivity screen. (A) Scatter dot plot of the library screening against HDAC11; arrows mark compounds selected for validation. (B) Summary of the resynthesized hits. (C) Dose–response curves for the resynthesized hits against HDAC1 and HDAC11, **trapoxin A** is used as positive control compound. (D) Structures of **14-N^{C6}OH** and its analogues and their potencies against HDAC11. (E) Selectivity profile of **14-N^{C6}OH** (1 μM) and **14-NHOH** (1 μM). The data in B–E represent mean ± standard deviation of at least two individual assays performed in duplicate.

in the selected hits were noncanonical amino acids and therefore our expansion of the chemical space appeared to be necessary to achieve potent inhibition (Figure 2A). At the C-terminus, the selected hits contained only acyclic aminothiols **AT1**, **AT2**, and **AT4**, which are more flexible and could possibly allow the macrocycles to adopt a more suitable conformation when interacting with the enzyme. All cyclization linkers were present in the selected hit series but with a higher frequency of the aromatic heterocycles **L4** and **L6** (Figure 2A). Of the 12 hits, seven were resynthesized, purified, and tested in dose–response experiments against HDACs 1 and 11, revealing that all, except compound **16-N^{C6}OH**, were selective inhibitors of HDAC11 (Figure 2B,C).

Macrocycle **14-N^{C6}OH** was the most potent hit with a K_i = 40 nM and was therefore selected for focused SAR evaluation. Thus, to address the role the N-alkylation of the hydroxamic acid for selectivity between the isozymes, we prepared a nonsubstituted hydroxamic acid analogue (**14-NHOH**) and an *N*-tetradecyl analogue (**14-N^{C14}OH**; to match the chain length of Kmyr) as well as a carboxylic acid analogue (**14-OH**) to probe the importance of a strong zinc-binding group. The compound **14-N^{C14}OH** (K_i = 50 nM) was equipotent to the original macrocycle against HDAC11, showing that the decision to reduce the lipophilicity of the building block from Asuha^{C14} to Asuha^{C6} had not compromised the power of the library to deliver selective inhibitors. Removal of the alkyl chain in **14-NHOH** (K_i = 1300 nM), on the other hand, caused a ∼ 30-fold decrease in potency against HDAC11 (Figure 2D and Supplementary Table S7), revealing a key role of the alkyl chain for potent inhibition of HDAC11. No inhibition was observed for **14-OH**, which validated the necessity for a strong chelating moiety for potent enzyme inhibition and, in turn, provided a compound that can be applied as a negative control in biochemical experiments. Next, the series of resynthesized compounds was profiled against HDAC1–9 to assess selectivity across other HDAC isozymes

https://doi.org/10.1021/jacsau.4c01148
JACS Au 2025, 5, 1299–1307

(Figure 2E, Supplementary Figure S10 and Supplementary Table S8). Compounds **14-N^{C6}OH** and **14-N^{C14}OH** exhibited no inhibition of HDAC1−9 at 1 μM concentration (Figure 2E) and only minor degree of inhibition (~20%) of HDAC1−3 at 10 μM. Thus, the alkyl chain of 6 carbon atoms provided excellent selectivity that was not improved by further extending its length. The nonsubstituted hydroxamate **14-NHOH**, on the other hand, inhibited HDACs 1−3, 6, and 8 at low nanomolar concentration, which further confirms the importance of the presence of an alkyl chain for achieving both potency against and selectivity for HDAC11 (Supplementary Figure S10 and Supplementary Table S8).

Furthermore, we observed limited aqueous solubility due to the high lipophilicity of the tetradecyl chain and **14-N^{C6}OH** was therefore selected for further investigations. Next, we assessed the ability of the macrocycle to inhibit demyristoylation in the more complex environment of a cell lysate. Though several sirtuin (SIRT) enzymes have been shown to exhibit Kmyr hydrolase activity,[30−36] SIRT2 and HDAC11 are the most efficient erasers of this posttranslational modification. Because SIRT2 requires the presence of nicotinamide adenine dinucleotide (NAD^+) as cosubstrate and is potently inhibited by a previously developed compound (**ALN-301**; Supplementary Figure S11),[37] we envisioned that the activities of the two hydrolases could be distinguished by using this inhibitor. However, because many immortalized cell lines exhibit very low expression levels of HDAC11, we first prepared cell lysate from HEK293T cells that overexpressed HDAC11 (Supplementary Figure S12). This lysate exhibited demyristoylase enzyme activity that was not affected by the SIRT2 inhibitor **ALN-301** but was completely inhibited by the nonselective HDAC inhibitor **trapoxin A**, which strongly suggests that HDAC11 is the enzyme responsible for the measured hydrolase activity against the Ac-ETDKmyr-AMC substrate. Further, this hydrolase activity was inhibited by **14-N^{C6}OH** at submicromolar concentration (Supplementary Figure S11). We then tested the ability of mouse brain lysate to remove the Kmyr modification of the same fluorogenic substrate Ac-ETDKmyr-AMC, because brain is one of the tissues with the highest expression of HDAC11. Our data show that the mouse brain lysate indeed contains HDAC11 (Supplementary Figure S13) and harbors demyristoylase activity that can be inhibited to 18% and 11% residual HDAC11 activity at 1 μM inhibitor concentration by **14-N^{C6}OH** and **14-N^{C14}OH**, respectively (Figure 3A). We also tested the lysate for deacetylase activity against the Ac-LGKac-AMC substrate (routinely used for HDACs 1−3, 6, and 8), and found that **14-N^{C6}OH** and **14-N^{C14}OH** allowed 59% and 74% residual HDAC activity at 5 μM inhibitor concentration and 87% and 92% HDAC activity at 1 μM under these conditions. On the other hand, the nonalkylated hydroxamate-containing compound **14-NHOH** was a potent inhibitor of deacetylation, giving 84% inhibition at 250 nM inhibitor concentration (Figure 3B). Together these experiments demonstrate potent and selective inhibition of HDAC11 by **14-N^{C6}OH** and **14-N^{C14}OH** but not by the nonalkylated compound **14-NHOH**, using both recombinant enzymes and HDAC activity in cell and tissue lysates.

With this potent and selective compound in hand, we envisioned that our macrocyclic scaffold could be modified to provide various bifunctional probes, and initially aimed to develop a biotin-labeled pulldown probe for evaluation of interaction partners of HDAC11 in different cells or tissues. To identify an exit vector for a linker, we synthesized three

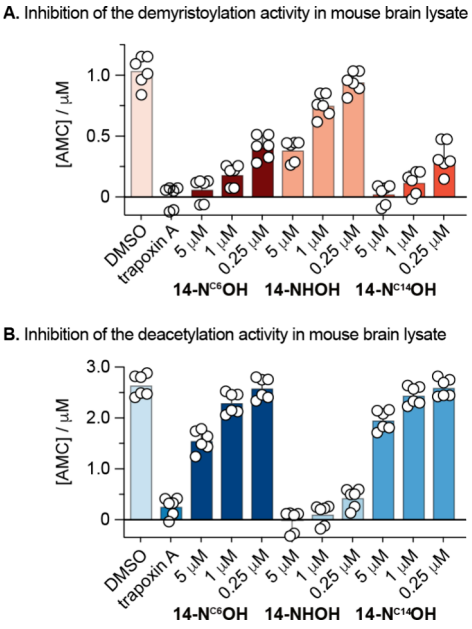

Figure 3. Activity of **14-N^{C6}OH** and analogues against enzymatic activities in mouse brain lysate. (A) Demyristoylation of the Ac-ETDKmyr-AMC substrate with mouse brain lysate. B) Deacetylation the Ac-LGKac-AMC substrate with mouse brain lysate. The data represent mean ± standard deviation of three individual assays performed in technical duplicate compared to DMSO as negative control. **Trapoxin A** was dosed at 1 μM concentration as positive control of nonselective inhibition of Zn^{2+}-dependent HDACs. AMC = 7-amino-4-methylcoumarin.

different alkyne-containing analogs of **14-N^{C6}OH**, which revealed retained potencies for compounds modified at the Phe(o-CF_3) and the pyridine positions but not at the isoleucine position (Supplementary Figure S14A).

We then prepared biotin-labeled versions of the two potent alkyne-containing macrocycles to give probes **18** and **19** (see the Supporting Information for full chemical structures), which also retained potency as HDAC11 inhibitors (Supplementary Figure S14B). Next, we loaded these onto magnetic streptavidin-coated beads and performed pulldown experiments from T-47D breast cancer cell lysate (Figure 4A). The T-47D cells were chosen because we had identified this cell line to exhibit higher expression of HDAC11 compared to a selection of other cell lines tested (Figure 4B). Gratifyingly, when performing the pulldown experiments with beads containing either probe **18** or probe **19**, we could detect native HDAC11 by Western blotting. Further, we could detect its only previously reported complex partner HDAC6,[4] and pulldown of both enzymes could be outcompeted by addition of free **14-N^{C6}OH** (Figure 4C). Because our macrocycle has poor affinity for HDAC6, these competition data confirm that HDAC6 and HDAC11 indeed interact with each other, either directly or through additional proteins, as previously indicated by coimmunoprecipitation experiments.[4] Thus, we anticipate that this probe should enable detailed chemo-proteomic HDAC inhibitor profiling in the future, including HDAC11, which has been challenging in the past.[38]

We then employed the chloroalkane penetration assay (CAPA) to assess the cell permeating properties of **14-N^{C6}OH**. CAPA reports on the ability of chloroalkane (CA)-labeled compounds to enter the cytosol of cells in culture, where they form a covalent bond to an expressed HaloTag construct

https://doi.org/10.1021/jacsau.4c01148
JACS Au 2025, 5, 1299−1307

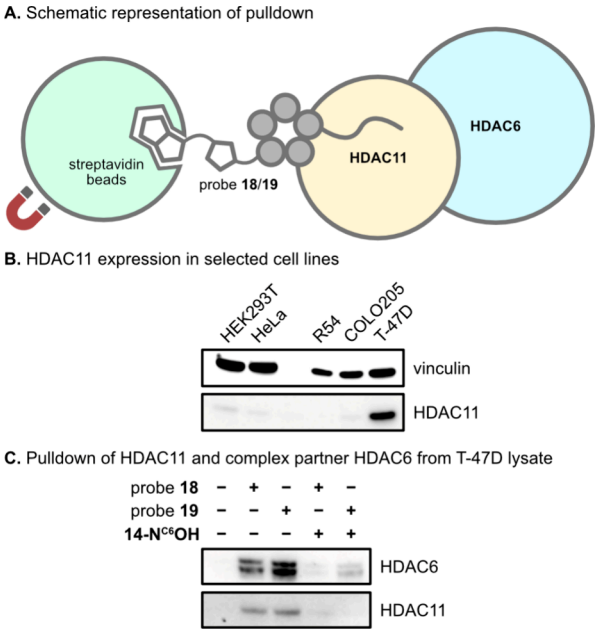

Figure 4. Pulldown of native HDAC11 and complex partner HDAC6 from cell lysate. (A) Cartoon illustration of the pulldown experiment, where the biotinylated probe (**18** or **19**) is preincubated with streptavidin-coated magnetic beads, followed by T-47D whole cell lysate. (B) Relative expression of HDAC11 in cell lysate (20 μg) from selected cultured cells to identify a suitable cell line for pulldown of native HDAC11. (C) Pulldown of HDAC11 and HDAC6 with probes **18** and **19** (50 μM) from T-47D cell lysate including competition with **14-N^{C6}OH** (10 μM) (n = 2). For synthesis and full structures of the probes, see Supporting Information [we note that probe **18** was only obtained with 77% purity based on analytical HPLC analysis (215 nm)]. For full blots and replicates, see Supplementary Figure S15.

(Figure 5A).[39] Performing dose−response experiments allow for the determination of "CP_{50} values", defined as the concentration of test compound at which a 50% reduction in fluorescence signal is observed under the assay conditions (Figure 5A). The assay usually requires the introduction of a chloroalkane moiety into the peptide via a short polyethylene glycol (PEG) chain. Thus, the standard CAPA tag adds 308 Da to the molecular weight of the compound of interest, which can significantly alter the properties of smaller peptides like **14-N^{C6}OH**. Here, the structural similarities between our N-hexylated Asuha moiety and the CA tag itself, led us to hypothesize that a minimal hydrogen to chloride atom substitution in the hexyl group would render the molecule amenable to HaloTag conjugation. To this end, we synthesized **14-N^{CA}OH** (+34 Da) and Ac-Asuha(CA)-Trp-NH_2 (**20**), an analogue of the commonly used positive control compound CA-Trp-NH_2 (**21**), and tested these probes using the standard CAPA procedure (Supplementary Figure S16).[39] Our results showed that **14-N^{CA}OH** is a highly cell permeating compound with CP_{50} of 94 nM while the Ac-Asuha(CA)-Trp-NH_2 (**20**) analogue showed 10-fold lower degree of permeation (Figure 5B), suggesting that the macrocycle is contributing to the degree of cell penetration. Compound **14-N^{CA}OH** was also tested for inhibition of HDAC11 and was found equipotent to the original inhibitor **14-N^{C6}OH**, highlighting the elegance of the minimal H → Cl substitution.

Though HDAC11 has been identified as a long-chain deacylase enzyme, several studies have suggested that it can also affect lysine acetylation in cells.[40−42] We therefore compared the effects of HDAC11 inhibitor **14-N^{C6}OH** and broad-acting HDAC inhibitors, **14-NHOH** and **trapoxin A**, on the levels of histone acetylation in cell culture. Following a 5 h treatment of HEK293T cells with **14-N^{C6}OH** (5 μM), we did not observe any measurable increase in global histone acetylation levels (Kac) nor at selected specific sites H3K18ac, H3K27ac, and H3K36ac by Western blot analysis (Figure 5C). The **14-NHOH** inhibitor, on the other hand, caused an increase in all the tested acetylation sites, demonstrating potent inhibition of class I HDAC activity, which underscores the difference in selectivity profile between the two compounds in a cellular context.

Finally, to evaluate in-cell activity of our HDAC11 inhibitor, we attempted to perform cellular thermal shift assays (CETSA) (Supplementary Figure S20) and iso-thermal dose−response fingerprint CETSA in T-47D cells, which did not provide reproducible data. Instead, we then treated T-47D and HEK293T cells with compound and subsequently performed Western blotting to assess the effects on the expression levels of yes-associated protein 1 (YAP1) and SOX2. These proteins have been previously shown to be regulated by HDAC11 in A549 lung adenocarcinoma cells,[43] and have been previously applied as markers for in-cell HDAC11 inhibition.[20] The levels of both proteins were significantly downregulated in response to the compound in a dose-dependent manner compared to the DMSO control, as expected based on previous reports[20,43] (Figure 5D). The same trend was observed in HEK293T cells (Supplementary Figure S21); albeit, to a lesser extent than in T-47D cells, which we speculate could be related to lower expression of HDAC11 in HEK293T cells. Further, the compound **14-N^{C6}OH** exhibited limited effect on the viability of both cell types as measured by MTT assays (Supplementary Figure S23), underscoring the potential to use this molecule as a probe for investigating the biology of HDAC11 in cell-based assays without encountering adverse toxic effects.

CONCLUSION

In this work, we pursued two different strategies for developing novel tool compounds that target HDAC11 in cells to enable investigation of the biological function of this enzyme. We initially attempted to use privileged natural product-derived peptide macrocycles as the starting point, which provided high potency but limited selectivity for HDAC11, when introducing *N*-alkylated hydroxamic acid moieties as zinc-binding groups. Instead, we combined these zinc-binding groups with de novo high-throughput macrocycle synthesis and screening against HDAC11, which furnished potent, selective, and cell-permeating inhibitors of the enzyme. Thus, our data suggest that using the *N*-alkylated hydroxamic acid motifs constitute general HDAC11-targeting motifs, but we also importantly find that the contribution of the macrocycle to the binding affinity determines the extent of selectivity achieved.

The selected hit macrocycle from our screen exhibited cell penetration in CAPA, using a minimally modified analogue (**14-N^{CA}OH**). In addition, we find that the nonalkylated hydroxamic acid analogue (**14-NHOH**) causes an increase in histone acetylation, while the **14-N^{C6}OH** causes an increase in HDAC11-regulated expression of YAP1 and SOX2 in cultured cells, in agreement with their selectivity profiles recorded against recombinant enzymes or the enzyme activity in mouse brain lysate.

https://doi.org/10.1021/jacsau.4c01148
JACS Au 2025, 5, 1299−1307

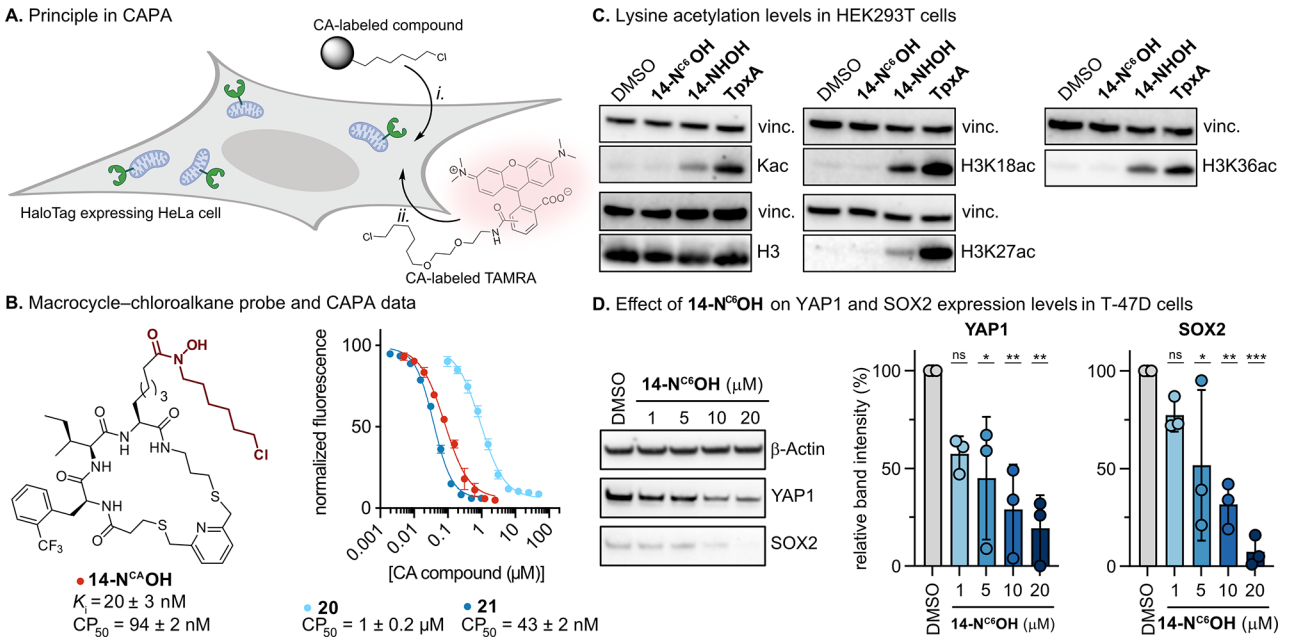

Figure 5. Cell penetration, histone acetylation, and HDAC11 regulated YAP1 and SOX2 expression. (A) Schematic of the principle in CAPA: cultured HaloTag-expressing HeLa cells are treated with CA-labeled test compound (*i*), followed by CA-TAMRA probe (*ii*), and flow cytometry is then applied to determine the extent of competition for CA conjugation sites inside the cells. (B) Structure of synthesized chloroalkane probe **14-N^{CA}OH** and CAPA results after 4 h treatment with compounds (n = 3). The data represent mean ± standard deviation of at least two individual assays performed in duplicate. See the Supporting Information for synthesis of **14-N^{CA}OH** and the positive control compounds, Ac-Asuha(CA)-Trp-NH$_2$ (**20**) and CA-Trp-NH$_2$ (**21**). (C) Histone acetylation levels following treatment of HEK293T cells with **14-N^{C6}OH** (5 μM), **14-NHOH** (5 μM), or **trapoxin A** (50 nM), with blots above each protein being vinculin (vinc.) used as the loading control (n = 2). For full blots and replicates, see Supplementary Figures S17–19. (D) Regulation of the expression of YAP1 and SOX2 by inhibiting HDAC11 in T-47D cells (n = 3). See Supplementary Figures S21–23 for data from HEK293T cells and full blots of all replicates. Statistical significance was calculated using one-way ANOVA tests with adjusted p values in comparison to treatment with DMSO: ns denotes $p > 0.05$, *$p < 0.05$, **$p < 0.01$, ***$p < 0.001$.

Our work provides general insights for the future design of probes targeting HDAC11, including ligands for potential drug discovery efforts. Our macrocyclic inhibitor, **14-N^{C6}OH**, and its derived biotin-labeled probes constitute tool compounds that we expect to be able to help elucidate the biology of HDAC11.

■ ASSOCIATED CONTENT

Supporting Information

The Supporting Information is available free of charge at https://pubs.acs.org/doi/10.1021/jacsau.4c01148.

Supplementary figures illustrating library quality control experiments and test reactions, dose–response curves and bar graphs for tested compounds, heatmap for library screening, and copies of full Western blots; Supplementary tables containing assay data, library compound sequences, library equipment and utilities, and library assay data; Experimental procedures, materials, methods, and compound characterization data; Copies of HPLC chromatograms as well as ^{1}H, ^{13}C, and ^{19}F NMR spectra; All peptide macrocycles were examined using the publicly accessible pan-assay interference compounds (PAINS) filter: ZINC 15 patterns search[44] (PDF)

■ AUTHOR INFORMATION

Corresponding Authors

Christian Heinis − *Institute of Chemical Sciences and Engineering, School of Basic Sciences, École Polytechnique Fédérale de Lausanne (EPFL), CH-1015 Lausanne, Switzerland;* orcid.org/0000-0001-9982-9457; Email: christian.heinis@epfl.ch

Christian A. Olsen − *Center for Biopharmaceuticals and Department of Drug Design and Pharmacology, Faculty of Health and Medical Sciences, University of Copenhagen, DK-2100 Copenhagen, Denmark;* orcid.org/0000-0002-2953-8942; Email: cao@sund.ku.dk

Authors

Daniela Danková − *Center for Biopharmaceuticals and Department of Drug Design and Pharmacology, Faculty of Health and Medical Sciences, University of Copenhagen, DK-2100 Copenhagen, Denmark;* Present Address: AstraZeneca AB R&D, Pepparedsleden 1, 43153 Gothenburg, Sweden; orcid.org/0000-0003-1957-3514

Alexander L. Nielsen − *Institute of Chemical Sciences and Engineering, School of Basic Sciences, École Polytechnique Fédérale de Lausanne (EPFL), CH-1015 Lausanne, Switzerland;* Present Address: Global Research Technologies, Novo Nordisk A/S, DK-2760 Måløv, Denmark.

Anne Zarda − *Institute of Chemical Sciences and Engineering, School of Basic Sciences, École Polytechnique Fédérale de Lausanne (EPFL), CH-1015 Lausanne, Switzerland*

Tobias N. Hansen − *Center for Biopharmaceuticals and Department of Drug Design and Pharmacology, Faculty of Health and Medical Sciences, University of Copenhagen, DK-2100 Copenhagen, Denmark;* orcid.org/0000-0001-6098-058X

https://doi.org/10.1021/jacsau.4c01148
JACS Au 2025, 5, 1299–1307

Marie Hesse − *Center for Biopharmaceuticals and Department of Drug Design and Pharmacology, Faculty of Health and Medical Sciences, University of Copenhagen, DK-2100 Copenhagen, Denmark*
Michaela Benová − *Center for Biopharmaceuticals and Department of Drug Design and Pharmacology, Faculty of Health and Medical Sciences, University of Copenhagen, DK-2100 Copenhagen, Denmark*
Athanasios Tsiris − *Center for Biopharmaceuticals and Department of Drug Design and Pharmacology, Faculty of Health and Medical Sciences, University of Copenhagen, DK-2100 Copenhagen, Denmark*
Christian R. O. Bartling − *Center for Biopharmaceuticals and Department of Drug Design and Pharmacology, Faculty of Health and Medical Sciences, University of Copenhagen, DK-2100 Copenhagen, Denmark*
Edward J. Will − *Institute of Chemical Sciences and Engineering, School of Basic Sciences, École Polytechnique Fédérale de Lausanne (EPFL), CH-1015 Lausanne, Switzerland*
Kristian Strømgaard − *Center for Biopharmaceuticals and Department of Drug Design and Pharmacology, Faculty of Health and Medical Sciences, University of Copenhagen, DK-2100 Copenhagen, Denmark;* orcid.org/0000-0003-2206-4737
Carlos Moreno-Yruela − *Center for Biopharmaceuticals and Department of Drug Design and Pharmacology, Faculty of Health and Medical Sciences, University of Copenhagen, DK-2100 Copenhagen, Denmark; Institute of Chemical Sciences and Engineering, School of Basic Sciences, École Polytechnique Fédérale de Lausanne (EPFL), CH-1015 Lausanne, Switzerland;* orcid.org/0000-0003-2450-6519

Complete contact information is available at: https://pubs.acs.org/10.1021/jacsau.4c01148

Author Contributions

CRediT: **Daniela Dankova** conceptualization, formal analysis, investigation, methodology, visualization, writing - original draft, writing - review & editing; **Alexander Lund Nielsen** conceptualization, formal analysis, investigation, methodology, supervision, visualization, writing - review & editing; **Anne Zarda** formal analysis, investigation, methodology; **Tobias N. Hansen** formal analysis, investigation, methodology, visualization, writing - review & editing; **Marie Hesse** formal analysis, investigation, methodology; **Michaela Benová** formal analysis, investigation, methodology; **Athanasios Tsiris** formal analysis, investigation, methodology; **Christian R. O. Bartling** formal analysis, investigation, methodology, writing - review & editing; **Edward Will** formal analysis, investigation, methodology; **Kristian Strømgaard** resources, supervision, writing - review & editing; **Carlos Moreno Yruela** conceptualization, formal analysis, investigation, methodology, supervision, visualization, writing - review & editing; **Christian Heinis** funding acquisition, resources, supervision, writing - review & editing; **Christian A. Olsen** conceptualization, formal analysis, funding acquisition, investigation, methodology, project administration, resources, supervision, visualization, writing - original draft, writing - review & editing.

Notes

The authors declare the following competing financial interest(s): EPFL has filed a PCT application covering parts of the presented library preparation method (WO/2022/242993) with A.L.N. and C.H. as co-inventors. C.H. is a co-founder of Orbis Medicines. The remaining authors declare no competing interests.

ACKNOWLEDGMENTS

We gratefully acknowledge financial support from the Independent Research Fund Denmark−Technical and Production Sciences (0136-00412B, C.A.O.) and the Novo Nordisk Foundation (NNF23OC0085899; C.A.O.). This project has received funding from the European Research Council (ERC) under the European Union's Horizon 2020 Research and Innovation Programme (grant agreement numbers: 101020521−TARGET, C.H.; 725172−SIRFUNCT, C.A.O.).

REFERENCES

(1) Moreno-Yruela, C.; Galleano, I.; Madsen, A. S.; Olsen, C. A. Histone Deacetylase 11 Is an ε-*N*-Myristoyllysine Hydrolase. *Cell Chem. Biol.* **2018**, *25*, 849−856.
(2) Kutil, Z.; Novakova, Z.; Meleshin, M.; Mikesova, J.; Schutkowski, M.; Barinka, C. Histone Deacetylase 11 Is a Fatty-Acid Deacylase. *ACS Chem. Biol.* **2018**, *13*, 685−693.
(3) Cao, J.; Sun, L.; Aramsangtienchai, P.; Spiegelman, N. A.; Zhang, X.; Huang, W.; Seto, E.; Lin, H. HDAC11 regulates type I interferon signaling through defatty-acylation of SHMT2. *Proc. Natl. Acad. Sci. U.S.A.* **2019**, *116*, 5487−5492.
(4) Gao, L.; Cueto, M. A.; Asselbergs, F.; Atadja, P. Cloning and Functional Characterization of HDAC11, a Novel Member of the Human Histone Deacetylase Family*. *J. Biol. Chem.* **2002**, *277*, 25748−25755.
(5) Yanginlar, C.; Logie, C. HDAC11 is a regulator of diverse immune functions. *Biochim. Biophys. Acta - Gene Regulatory Mechanisms* **2018**, *1861*, 54−59.
(6) Villagra, A.; Cheng, F.; Wang, H. W.; Suarez, I.; Glozak, M.; Maurin, M.; Nguyen, D.; Wright, K. L.; Atadja, P. W.; Bhalla, K.; Pinilla-Ibarz, J.; Seto, E.; Sotomayor, E. M. The histone deacetylase HDAC11 regulates the expression of interleukin 10 and immune tolerance. *Nat. Immunol.* **2009**, *10*, 92−100.
(7) Cheng, F.; Lienlaf, M.; Perez-Villarroel, P.; Wang, H. W.; Lee, C.; Woan, K.; Woods, D.; Knox, T.; Bergman, J.; Pinilla-Ibarz, J.; Kozikowski, A.; Seto, E.; Sotomayor, E. M.; Villagra, A. Divergent roles of histone deacetylase 6 (HDAC6) and histone deacetylase 11 (HDAC11) on the transcriptional regulation of IL10 in antigen presenting cells. *Mol. Immunol.* **2014**, *60*, 44−53.
(8) Bagchi, R. A.; Ferguson, B. S.; Stratton, M. S.; Hu, T.; Cavasin, M. A.; Sun, L.; Lin, Y.-H.; Liu, D.; Londono, P.; Song, K.; et al. HDAC11 suppresses the thermogenic program of adipose tissue via BRD2. *JCI Insight* **2018**, *3*, 3.
(9) Shook, B. V.; Noonepalle, A.; Satish, K. R.; Hernandez, M. Compositions for and methods of treating a subject having inflammation. WO 2023/146860 A1, 2023.
(10) Roche, J.; Bertrand, P. Inside HDACs with more selective HDAC inhibitors. *Eur. J. Med. Chem.* **2016**, *121*, 451−483.
(11) Shortt, J.; Ott, C. J.; Johnstone, R. W.; Bradner, J. E. A chemical probe toolbox for dissecting the cancer epigenome. *Nat. Rev. Cancer* **2017**, *17*, 160−183.
(12) Ho, T. C. S.; Chan, A. H. Y.; Ganesan, A. Thirty Years of HDAC Inhibitors: 2020 Insight and Hindsight. *J. Med. Chemi.* **2020**, *63*, 12460−12484.
(13) Kijima, M.; Yoshida, M.; Sugita, K.; Horinouchi, S.; Beppu, T. Trapoxin, an antitumor cyclic tetrapeptide, is an irreversible inhibitor of mammalian histone deacetylase. *J. Biol. Chem.* **1993**, *268*, 22429−22435.
(14) Taunton, J.; Hassig, C. A.; Schreiber, S. L. A mammalian histone deacetylase related to the yeast transcriptional regulator Rpd3p. *Science* **1996**, *272*, 408−411.

(15) Darkin-Rattray, S. J.; Gurnett, A. M.; Myers, R. W.; Dulski, P. M.; Crumley, T. M.; Allocco, J. J.; Cannova, C.; Meinke, P. T.; Colletti, S. L.; Bednarek, M. A.; Singh, S. B.; Goetz, M. A.; Dombrowski, A. W.; Polishook, J. D.; Schmatz, D. M. Apicidin: a novel antiprotozoal agent that inhibits parasite histone deacetylase. *Proc. Natl. Acad. Sci. U.S.A.* **1996**, *93*, 13143−13147.
(16) Furumai, R.; Komatsu, Y.; Nishino, N.; Khochbin, S.; Yoshida, M.; Horinouchi, S. Potent histone deacetylase inhibitors built from trichostatin A and cyclic tetrapeptide antibiotics including trapoxin. *Proc. Natl. Acad. Sci. U.S.A.* **2001**, *98*, 87−92.
(17) Maolanon, A. R.; Kristensen, H. M. E.; Leman, L. J.; Ghadiri, M. R.; Olsen, C. A. Natural and Synthetic Macrocyclic Inhibitors of the Histone Deacetylase Enzymes. *ChemBioChem.* **2017**, *18*, 5−49.
(18) Kitir, B.; Maolanon, A. R.; Ohm, R. G.; Colaco, A. R.; Fristrup, P.; Madsen, A. S.; Olsen, C. A. Chemical Editing of Macrocyclic Natural Products and Kinetic Profiling Reveal Slow, Tight-Binding Histone Deacetylase Inhibitors with Picomolar Affinities. *Biochemistry* **2017**, *56*, 5134−5146.
(19) Son, S. I.; Cao, J.; Zhu, C. L.; Miller, S. P.; Lin, H. Activity-Guided Design of HDAC11-Specific Inhibitors. *ACS Chem. Biol.* **2019**, *14*, 1393−1397.
(20) Ho, T. T.; Peng, C.; Seto, E.; Lin, H. Trapoxin A Analogue as a Selective Nanomolar Inhibitor of HDAC11. *ACS Chem. Biol.* **2023**, *18*, 803−809.
(21) Bieliauskas, A. V.; Weerasinghe, S. V.; Negmeldin, A. T.; Pflum, M. K. Structural Requirements of Histone Deacetylase Inhibitors: SAHA Analogs Modified on the Hydroxamic Acid. *Arch. Pharm.* **2016**, *349*, 373−382.
(22) Moreno-Yruela, C.; Bæk, M.; Vrsanova, A. E.; Schulte, C.; Maric, H. M.; Olsen, C. A. Hydroxamic acid-modified peptide microarrays for profiling isozyme-selective interactions and inhibition of histone deacetylases. *Nat. Commun.* **2021**, *12*, 62.
(23) Schuttel, M.; Will, E.; Sangouard, G.; Zarda, A.; Habeshian, S.; Nielsen, A. L.; Heinis, C. Solid-phase peptide synthesis in 384-well plates. *J. Pept. Sci.* **2024**, *30*, No. e3555.
(24) Nielsen, A. L.; Bognar, Z.; Mothukuri, G. K.; Zarda, A.; Schuttel, M.; Merz, M. L.; Ji, X.; Will, E. J.; Chinellato, M.; Bartling, C. R. O.; et al. Large Libraries of Structurally Diverse Macrocycles Suitable for Membrane Permeation. *Angew. Chem., Int. Ed.* **2024**, *63*, No. e202400350.
(25) Bognar, Z.; Mothukuri, G. K.; Nielsen, A. L.; Merz, M. L.; Pânzar, P. M. F.; Heinis, C. Solid-phase peptide synthesis on disulfide-linker resin followed by reductive release affords pure thiol-functionalized peptides. *Org. Biomol. Chem.* **2022**, *20*, 5699−5703.
(26) Merz, M. L.; Habeshian, S.; Li, B.; David, J. G. L.; Nielsen, A. L.; Ji, X.; Il Khwildy, K.; Duany Benitez, M. M.; Phothirath, P.; Heinis, C. De novo development of small cyclic peptides that are orally bioavailable. *Nat. Chem. Biol.* **2024**, *20*, 624.
(27) Nolan, M. D.; Schüttel, M.; Scanlan, E. M.; Nielsen, A. L. Nanomole-scale photochemical thiol-ene chemistry for high-throughput late-stage diversification of peptide macrocycles. *Peptide. Sci.* **2024**, e24310.
(28) Kutil, Z.; Mikesova, J.; Zessin, M.; Meleshin, M.; Novakova, Z.; Alquicer, G.; Kozikowski, A.; Sippl, W.; Barinka, C.; Schutkowski, M. Continuous Activity Assay for HDAC11 Enabling Reevaluation of HDAC Inhibitors. *ACS Omega* **2019**, *4*, 19895−19904.
(29) Moreno-Yruela, C.; Olsen, C. A. High-throughput screening of histone deacetylases and determination of kinetic parameters using fluorogenic assays. *STAR Protoc.* **2021**, *2*, 100313.
(30) Jiang, H.; Khan, S.; Wang, Y.; Charron, G.; He, B.; Sebastian, C.; Du, J.; Kim, R.; Ge, E.; Mostoslavsky, R.; Hang, H. C.; Hao, Q.; Lin, H. SIRT6 regulates TNF-alpha secretion through hydrolysis of long-chain fatty acyl lysine. *Nature* **2013**, *496*, 110−113.
(31) Feldman, J. L.; Baeza, J.; Denu, J. M. Activation of the protein deacetylase SIRT6 by long-chain fatty acids and widespread deacylation by mammalian sirtuins. *J. Biol. Chem.* **2013**, *288*, 31350−31356.
(32) Madsen, A. S.; Andersen, C.; Daoud, M.; Anderson, K. A.; Laursen, J. S.; Chakladar, S.; Huynh, F. K.; Colaco, A. R.; Backos, D. S.; Fristrup, P.; Hirschey, M. D.; Olsen, C. A. Investigating the Sensitivity of NAD+-dependent Sirtuin Deacylation Activities to NADH. *J. Biol. Chem.* **2016**, *291*, 7128−7141.
(33) Tong, Z.; Wang, Y.; Zhang, X.; Kim, D. D.; Sadhukhan, S.; Hao, Q.; Lin, H. SIRT7 Is Activated by DNA and Deacetylates Histone H3 in the Chromatin Context. *ACS Chem. Biol.* **2016**, *11*, 742−747.
(34) Tong, Z.; Wang, M.; Wang, Y.; Kim, D. D.; Grenier, J. K.; Cao, J.; Sadhukhan, S.; Hao, Q.; Lin, H. SIRT7 Is an RNA-Activated Protein Lysine Deacylase. *ACS Chem. Biol.* **2017**, *12*, 300−310.
(35) Wang, W. W.; Angulo-Ibanez, M.; Lyu, J.; Kurra, Y.; Tong, Z.; Wu, B.; Zhang, L.; Sharma, V.; Zhou, J.; Lin, H.; Gao, Y. Q.; Li, W.; Chua, K. F.; Liu, W. R. A Click Chemistry Approach Reveals the Chromatin-Dependent Histone H3K36 Deacylase Nature of SIRT7. *J. Am. Chem. Soc.* **2019**, *141*, 2462−2473.
(36) Bolding, J. E.; Nielsen, A. L.; Jensen, I.; Hansen, T. N.; Ryberg, L. A.; Jameson, S. T.; Harris, P.; Peters, G. H. J.; Denu, J. M.; Rogers, J. M.; Olsen, C. A. Substrates and Cyclic Peptide Inhibitors of the Oligonucleotide-Activated Sirtuin 7. *Angew. Chem., Int. Ed.* **2023**, *62*, No. e202314597.
(37) Nielsen, A. L.; Rajabi, N.; Kudo, N.; Lundø, K.; Moreno-Yruela, C.; Bæk, M.; Fontenas, M.; Lucidi, A.; Madsen, A. S.; Yoshida, M.; Olsen, C. A. Mechanism-based inhibitors of SIRT2: structure-activity relationship, X-ray structures, target engagement, regulation of α-tubulin acetylation and inhibition of breast cancer cell migration. *RSC Chem. Biol.* **2021**, *2*, 612−626.
(38) Lechner, S.; Malgapo, M. I. P.; Gratz, C.; Steimbach, R. R.; Baron, A.; Ruther, P.; Nadal, S.; Stumpf, C.; Loos, C.; Ku, X.; Prokofeva, P.; Lautenbacher, L.; Heimburg, T.; Wurf, V.; Meng, C.; Wilhelm, M.; Sippl, W.; Kleigrewe, K.; Pauling, J. K.; Kramer, K.; Miller, A. K.; Pfaffl, M. W.; Linder, M. E.; Kuster, B.; Medard, G. Target deconvolution of HDAC pharmacopoeia reveals MBLAC2 as common off-target. *Nat. Chem. Biol.* **2022**, *18*, 812−820.
(39) Peraro, L.; Deprey, K. L.; Moser, M. K.; Zou, Z.; Ball, H. L.; Levine, B.; Kritzer, J. A. Cell Penetration Profiling Using the Chloroalkane Penetration Assay. *J. Am. Chem. Soc.* **2018**, *140*, 11360−11369.
(40) Leslie, P. L.; Chao, Y. L.; Tsai, Y.-H.; Ghosh, S. K.; Porrello, A.; Van Swearingen, A. E. D.; Harrison, E. B.; Cooley, B. C.; Parker, J. S.; Carey, L. A.; Pecot, C. V. Histone deacetylase 11 inhibition promotes breast cancer metastasis from lymph nodes. *Nat. Commun.* **2019**, *10*, 4192.
(41) Heim, C. E.; Bosch, M. E.; Yamada, K. J.; Aldrich, A. L.; Chaudhari, S. S.; Klinkebiel, D.; Gries, C. M.; Alqarzaee, A. A.; Li, Y.; Thomas, V. C.; Seto, E.; Karpf, A. R.; Kielian, T. Lactate production by Staphylococcus aureus biofilm inhibits HDAC11 to reprogramme the host immune response during persistent infection. *Nat. Microbiol.* **2020**, *5*, 1271−1284.
(42) He, L.; Chen, Y.; Lin, S.; Shen, R.; Pan, H.; Zhou, Y.; Wang, Y.; Chen, S.; Ding, J. Regulation of Hsa-miR-4639−5p expression and its potential role in the pathogenesis of Parkinson's disease. *Aging Cell* **2023**, *22*, No. e13840.
(43) Bora-Singhal, N.; Mohankumar, D.; Saha, B.; Colin, C. M.; Lee, J. Y.; Martin, M. W.; Zheng, X.; Coppola, D.; Chellappan, S. Novel HDAC11 inhibitors suppress lung adenocarcinoma stem cell self-renewal and overcome drug resistance by suppressing Sox2. *Sci. Rep.* **2020**, *10*, 4722.
(44) Sterling, T.; Irwin, J. J. ZINC 15-Ligand Discovery for Everyone. *J. Chem. Inf. Model.* **2015**, *55*, 2324−2337.

https://doi.org/10.1021/jacsau.4c01148
JACS Au 2025, 5, 1299−1307